American Mineralogist, Volume 71, pages 1247–1257, 1986

Scanning Auger microscopy as a high-resolution microprobe for geologic materials

Michael F. Hochella, Jr.
Department of Geology, Stanford University, Stanford, California 94305, U.S.A.
David W. Harris, Arthur M. Turner
Physical Electronics Laboratories, Perkin-Elmer Corporation, 1161-C San Antonio Road, Mountain View, California 94043, U.S.A.

Abstract

We present in this study the groundwork necessary for the utilization of scanning Auger microscopy (SAM) as a high-resolution microprobe for geologic materials. The attributes of SAM that allow it to be a useful microanalytic tool for rocks are discussed and demonstrated. The technique is suitable for semiquantitative probing of <1-μm grains in rocks as well as performing surface studies with very high lateral resolution.

SAM analyses of feldspar surfaces suggest that the depth of Auger analysis is sufficient to measure representative bulk chemistries from relatively clean surfaces of crystalline silicates. It is shown that very light sputtering, used to eliminate thin contaminant surface layers due to air exposure and/or solvent residues, should not affect semiquantitative chemical analysis. It is also shown that elements as light as Li can be detected in minerals with SAM. Sample charging and degradation can be reduced and/or eliminated by using a beam voltage of 3 keV and currents in the low nanoampere range impinging on tilted specimens that are relatively clean. To demonstrate the technique, we describe an example of performing a semiquantitative chemical analysis of a <1-μm grain in a rock with chemical lateral resolution slightly better than 1 μm.

SAM is also briefly compared with other microanalysis techniques commonly used today, namely EPMA, SEM/EDS, and STEM/EDS. In comparison, the major disadvantage of SAM is sample charging and the fact that it is sensitive to electron-beam-stimulated surface degradation. The major advantage of SAM over these techniques is a combination of high lateral and depth analytic resolution and ease of light-element detection.

Introduction

Chemical microanalysis has become an invaluable tool to mineralogists and petrologists, particularly in the past 20 years, following the development of the first electron-probe microanalyzer (EPMA) by Castaing and Guinier in 1949 (see Castaing, 1960, for a review of their early work). Important related techniques developed since this time are analytical electron microscopy (AEM or STEM/EDS) and SEM/EDS, which combine energy-dispersive X-ray spectroscopy (EDS) with scanning transmission-electron microscopy (STEM) or secondary electron spectroscopy (SEM), respectively. Particularly in the last decade, scanning Auger microscopy (SAM) has come on the scene as yet another important addition to the chemical microanalysis field. Scanning Auger microprobes have the ability to perform semiquantitative elemental analysis on volumes several orders of magnitude smaller than those analyzed with EPMA or SEM/EDS.

The history of the development of SAM, which evolved from Auger electron spectroscopy (AES), began in 1922 when Pierre Auger detected the ejection of characteristic electrons (later named Auger electrons) from Ar atoms being bombarded by X-rays in a cloud chamber (see Auger, 1975, for a review of his early work). Ruthemann (1942), Hillier (1943), and Lander (1953) were among the first to show that characteristic Auger electrons could be stimulated from thin films and solids when struck by an electron beam. Unfortunately, efficient, high-resolution electron-energy analyzers were not available at the time, and high vacuum systems had yet to be perfected. Palmberg et al. (1969) described the first practical AES system, the basic concepts of which are still in use today. The key to their system was the cylindrical-mirror electron-energy analyzer. This highly efficient dispersive analyzer also has acceptable energy resolution, and its use made AES a practical analytical technique. SAM, which is AES performed with a focused scanning electron beam, soon followed these developments and was first performed on modified SEM's fitted with electron-energy analyzers (see Wells and Bremer, 1969, and MacDonald, 1970). Today, scanning Auger microprobes are generally tailored for surface analytic instruments operating under ultrahigh vacuum conditions with secondary electron detectors added for SEM imaging.

Applications of AES/SAM generally involve the near-surface analysis of conductors and semiconductors. For example, AES/SAM has found wide ranging applicability in

0003–004X/86/0910–1247$02.00

the microelectronics field (Holloway, 1980; Lowry and Hogrefe, 1980; Olson et al., 1983; Harris, 1984) and in various aspects of the metallurgical and chemical industries (see Joshi et al., 1975, and Holm, 1982, for reviews). On the other hand, the application of AES/SAM to insulating materials has been substantially limited due to charging problems and the degradational surface effects of electron beams. These effects include field-induced migration of mobile ions, beam heating, and electron-stimulated desorption and adsorption. However, these problems, in a number of cases, can be overcome or minimized, and AES has been used, for example, to study corrosion of silicate glass surfaces (see Pantano et al., 1975, and Pantano, 1981). Poppa and Elliot (1971) may have been the first to apply AES to minerals in a study of the (001) surface of muscovite which was used for epitaxial vapor deposition studies. The surfaces of quartz and vitreous silica have also been thoroughly examined by AES, with special emphasis on the problems of electron-induced surface degradation at high beam currents (Chang, 1971; Carriere et al., 1973; Carriere and Lang, 1977). Morrison et al. (1970), Connell et al. (1971), Gold et al. (1974, 1975), Grant et al. (1974), and Baron et al. (1977) were among the first to use AES in geologic investigations in studies involving the surface characterization of lunar dust. Since this time, Perry et al. (1982a, 1982b, 1983a, 1983b, 1984a, 1984b) have studied metal-ion interaction on and weathering of feldspar and sulfide surfaces with AES/SAM, and Remond et al. (1981, 1982, 1983, 1985) have used SAM to investigate how surface preparation of polished sections can affect optical measurements (color and reflectance) on sulfide minerals. More recently, Mucci et al. (1985) and Mucci and Morse (1985) have used AES to study adsorbed layers on carbonates after reaction with seawater, and White and Yee (1985) have used AES, X-ray photoelectron spectroscopy (XPS), and secondary-ion mass spectroscopy (SIMS) to study the surfaces of Fe^{2+}-containing minerals in contact with various aqueous solutions. Also, Mackinnon and Mogk (1985) and Mogk et al. (1985) have used SAM to study the near-surface composition of particulates collected from the stratosphere, and Bisdom et al. (1985) have used SAM and energy-dispersive X-ray analysis to study soil samples. Many of these studies have taken advantage of the depth-profile analyses obtainable with AES, which are typically superior to those that can be obtained with wide-area XPS. However, the potential use of the ultrahigh lateral resolution that can currently be achieved with AES/SAM has not been thoroughly explored for insulating materials.

In this first in a series of papers, we present the background necessary to effectively utilize SAM as a high-resolution microprobe to perform semiquantitative chemical analyses on <1-μm grains in rocks as has been demonstrated by Hochella (1985) and Hochella et al. (1985, 1986). The same principles can be used to study altered mineral surfaces on a <1-μm lateral scale. We include here a brief review of the fundamental principles of Auger spectroscopy, a discussion of near-surface vs. bulk analysis, light-element-detection and spatial-resolution capabilities of SAM, overcoming or minimizing problems associated with electron-beam-stimulated sample charging and degradation, and the quantitative nature of the technique. We will then describe a typical example of the analysis of a <1-μm mineral grain in a rock. Finally, we will compare SAM with other microanalysis instruments currently in use. In future papers in this series, we will report Auger sensitivity factors specifically derived for silicates (see Quantification section below) and present several applications of high-resolution SAM analyses to geologic problems.

SAM AS A MICROPROBE

Basic principles and instrument used

AES is a near-surface analytic technique in which, typically, an electron beam is used to excite Auger electrons from a solid. The inelastic mean free path of Auger electrons from inorganic solids in the energy range typically detected (0–2000 eV) is between approximately 4 and 20 Å depending on their energy (see, e.g., Seah and Dench, 1979, and Powell, 1984, and references therein), and significant Auger intensity comes from 2 to 3 times this depth. The Auger electron is produced when an atom undergoes an inner-shell ionization by X-ray or electron bombardment. The inner-shell vacancy can be filled by an electron from a higher energy level, and the energy released in this deexcitation process can result in the emission of an X-ray photon (the basis for X-ray fluorescence spectroscopy) or the ejection of a third electron, the Auger electron. As an example of the Auger process, Figure 1 schematically shows the three most probable Auger transitions that occur for Si.

In simplified terms, Auger electron energies can be calculated with the equation

$$E(VXY) = E(V) - E(X) - E(Y')$$

first proposed by Burhop (1952), where E(VXY) is the energy of the Auger electron of interest and the atomic shells involved in the Auger process are V, X, and Y (X and Y can also be the valence level). E(V) is the energy of the electronic level in which a core hole is created by an incoming photon or electron. E(X) is the energy of the electronic level in the same atom from which an electron falls to fill the core vacancy. E(V) and E(X) are energy levels with the atom in a singly ionized state, and they can be closely approximated by measuring the binding energies of electrons in these levels with photoelectron spectroscopy. E(Y) is the energy of the electronic level from which the Auger electron is derived, and E(Y′) is the energy of this level with the atom in an Auger transition–imposed doubly ionized state. E(Y′) can be approximated by a modified binding energy of this electronic level. This modification, first proposed by Shirley (1972), takes into account the relaxation of orbitals toward the hole in shell X and is called the atomic relaxation energy.

Because all elements have a unique set of electron-binding energies, all elements detectable by AES have a unique

Auger spectrum. This spectrum for a single element can be very complex, especially for the heavier elements. The number and energy distribution of Auger peaks for each element are dependent on (1) the permissible electronic transitions from X to V and (2) those electrons with energy E(Y′) such that

$$E(V) - E(X) > E(Y').$$

Fortunately, Auger transition probabilities are such that most elements have no more than four relatively intense Auger lines, and many have only two or three. It should also be noted that the exact Auger peak positions and shapes may include useful valence-state or chemical-environment information (see, e.g., Wagner et al., 1982).

The assignment of Auger lines is generally made empirically using Auger spectra derived from pure elements or simple compounds (Davis et al., 1976). On the other hand, theoretical (both relativistic and nonrelativistic) and semi-empirical calculations of Auger-line energies have generally been successful, agreeing with experimental values to within a few electron volts (see Thompson et al., 1985, and references therein). Tabulations of calculated Auger-line energies for all possible transitions, such as that found in Coghlan and Clausing (1971) or Larkins (1977), can be very helpful in sorting out complex spectra or very weak lines.

The three-electron Auger process precludes the detection of H and He. All other elements are detectable, although Li is only detectable by AES in condensed matter (see, e.g., Ohuchi et al., 1979, and Schowengerdt and Forrest, 1983, for Li analyses using AES). In the atomic state, Li would not be predicted to have Auger-electron emission because the 2*s* to 1*s* transitional energy is not large enough to eject the remaining 1*s* electron. However, in Li-containing solids, low-energy Auger lines are observed due to Li valence electrons that are low enough in binding energy to be ejected by the energy released from the 2*s* to 1*s* transition.

One fundamental drawback of Auger spectroscopy is that the inelastically backscattered primary electrons create a very intense background; because the characteristic Auger peaks are generally small relative to this background, the signal-to-noise ratio is often poor. In order to allow detection of weak and/or broad lines, it is common practice to plot the first derivative of a direct Auger spectrum (cf. electron paramagnetic-resonance spectra). Differentiated plots can be obtained electronically while data is being collected (with a lock-in amplifier) or by computer differentiation of stored direct spectra. Auger spectra presented in this paper have been computer differentiated and smoothed. If the Auger peak shapes in the direct spectrum remain similar between standard and unknown, the distance between the positive and negative excursions of the differentiated peaks (called peak-to-peak heights) are then used in semiquantitative Auger chemical analysis as has been justified by Seah (1979). More details on the principles and practice of AES/SAM can be found in reviews by, for example, Joshi et al. (1975) and Riviere (1983).

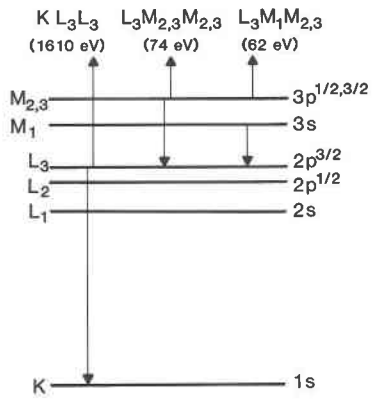

Fig. 1. Schematic diagram of the electron energy levels for Si showing the three Auger transitions that result in the most intense spectral lines. The transitions are labeled according to the electron level of the initial vacancy, the initial level of the hole-filling electron, and the level from which the Auger electron originates. The energies shown for these Auger electrons are taken from a quartz spectrum.

The instrument used in this study was the Perkin-Elmer Phi 600 SAM, a dedicated SAM instrument with attached secondary-electron detector for SEM imaging. This instrument has an electromagnetically focused electron gun mounted down the center of a single-pass cylindrical-mirror electron-energy analyzer (CMA) as shown in Figure 3 of Riviere (1983). This coaxial geometry has the advantage of reducing shadowing problems on rough surfaces. The CMA has a large electron-acceptance solid angle and is a very efficient analyzer for AES/SAM. The electron gun in the Phi 600 is capable of producing a beam as small as 0.035 μm in diameter at 10 keV and 0.05-nA beam current. Beam conditions used for insulating samples are given below.

Near-surface vs. bulk analysis

AES/SAM is generally regarded as a "surface" analytic instrument, whereas the electron-probe microanalyzer measures "bulk" chemistry. In most usages, though, "surface" and "bulk" are defined arbitrarily. There are surface techniques (scanning tunneling microscopy, electron-energy-loss spectroscopy, ion-scattering spectroscopy, etc.) that give information exclusively from the top monolayer of atoms on the surface. The near-surface of a solid includes the surface and several monolayers beneath it, on the order of a few tens of ångströms deep, the maximum measuring depth of AES and XPS. The electron microprobe analyzes the surface down to as deep as approximately 0.3 to 3 μm for oxides, depending on the electron-beam accelerating potentials typically used (5–15 keV). Even an analysis this deep may not be as representative of the true bulk as might be obtained by other methods (e.g., wet-chemical or X-ray fluorescence analysis). Generally, however, if the chemistry derived from the electron microprobe is going to compare to that derived from Auger spectroscopy, the near-surface chemistry must be repre-

Table 1. Peak-to-peak heights (in arbitrary units) from differentiated Auger spectra for the components of two feldspar standards

	Sri Lanka alkali feldspar	
	UHV fractured surface	Prepared surface*
O	57	57
Na	5	5
Al	5	6
Si	8	8
K	25	24
	Zillertal, Austria, albite	
	(010) surface	(001) surface
O	70	72
Na	13	10
Al	7	8
Si	10	10

* See text for a description of this surface preparation.

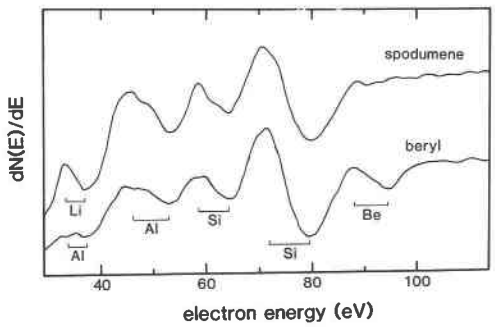

Fig. 2. Differentiated AES spectra showing the primary Li line for spodumene and the primary Be line for beryl. Note that a weak Al line, as seen in the beryl spectrum at approximately 37 eV, interferes with the Li line in the spodumene spectrum.

sentative of the bulk chemistry. This is obviously not always the case, and when SAM is used as a "microprobe," it is important to consider the potential difference between near-surface and bulk chemistries due to oxidation, corrosion (or weathering), chemical exchange, or atmospheric contamination.

All oxide, silicate, sulfide, and sulfate surfaces prepared outside of an ultrahigh vacuum environment that we have observed invariably show excess C and O in the Auger spectrum compared to any bulk measurement. Although AES cannot detect H, we presume that it is also on most surfaces, and occasionally we also observe very small amounts of N. The excess of these elements on surfaces is due to (1) the adsorption of CO_2, CO, H_2O, and perhaps various hydrocarbons from air exposure and (2) organic residues left from surface cleaning with organic solvents (see, e.g., Stephenson and Binkowski, 1976). We have shown that these surface contaminants should not typically interfere with near-surface semiquantitative analysis by AES/SAM. Table 1 shows the peak-to-peak heights from two Auger spectra of an alkali feldspar. One spectrum was taken on a surface immediately after it was exposed by fracturing in the low 10^{-9} torr vacuum of the SAM instrument. The other was taken on a surface exposed to air, boiled for 2 min each in acetone and ethanol, inserted into the SAM, and then sputtered with 4 keV Ar^+ ions for 10 s in an attempt to remove only the cleaning solvent residue. The two analyses are identical within the present analytic accuracy of the technique.

However, because of the depth resolution of AES, the question arises as to whether the technique can measure deep enough to obtain a representative chemistry from crystalline materials even on a relatively clean surface. As a test of this, we collected Auger spectra from the (010) crystal face and (001) cleavage face of the same albite single crystal. This phase and these faces were chosen because the structure viewed along **b*** and **c*** and the repeat distance in these directions in the feldspar structure are substantially different. The two analyses, tabulated in Table 1, show a discrepancy only for Na. We attribute this to the mobility of Na in these materials and the fact that the apparent Na content is very sensitive to the exact electron-beam conditions and sample tilt angle (see below). Overall, the results in Table 1 indicate that AES, at least in this case, is sampling enough of the near-surface region to obtain a representative chemistry for the entire crystal.

Light-element sensitivities

The detectability limit for an element with AES depends on the Auger transition probability and the mean free path of the Auger electron. Although under favorable conditions AES has a detection limit for a number of elements in the neighborhood of 0.1 at.% or better (see, e.g., Cazaux, 1984, and Shaffner and Keenan, 1983), certain elements, including the lightest elements detectable, Li and Be, have higher detection limits (see, e.g, the sensitivity-factor tables in Davis et al., 1976).

In order to test the detectability for Li and Be in common minerals that contain them as a major component, we collected high-energy-resolution AES spectra from single crystals of spodumene and beryl that contain approximately 10 at.% Li and Be, respectively. The differentiated spectra are shown in Figure 2. The Be signal in the beryl spectrum is well above noise level and could be used for semiquantitative analysis. On the other hand, the Li signal in the spodumene spectrum could not be used for quantification. This is because the major Li Auger transition at 37 eV is directly overlapping a weak Al Auger line in this spectrum. We estimate that up to a third of the apparent Li signal in this spectrum may be due to Al.

Considering the remaining second-row elements, detection of B is slightly better than that for Be, and the detection for C through Ne is substantially better, this according to empirical relative Auger sensitivity factors for these elements (Davis et al., 1976). In Auger spectra of silicate and oxide minerals, the oxygen line at approximately 503 eV will typically be the most intense line in

the spectrum because of both its relatively high atomic concentration and Auger sensitivity factor.

Spatial-resolution capabilities

Although the escape depth of characteristic Auger electrons is no more than a few tens of ångströms, the spatial resolution for AES/SAM still suffers from broadening phenomena. This reduction in spatial resolution has been discussed by Janssen and Venables (1978), El Gomati and Prutton (1978), El Gomati et al. (1979), and Cazaux (1983), among others. Broadening is due to three principle factors: (1) Auger electron emission from scattered primary electrons in the solid, (2) Auger electron emission from the near-surface due to backscattered electrons, and (3) Auger electron emission produced from both characteristic X-rays and Bremsstrahlung. The second factor is by far the most serious compromising factor to the spatial resolution of AES/SAM. However, despite this, a lateral analytic resolution of 0.03 μm has been demonstrated for SAM in conductors (see, e.g., Venables et al., 1976). Modeling of backscattering by Monte Carlo calculations has shown that chemical resolution for SAM should be roughly twice the diameter of the beam outline on the surface (El Gomati and Prutton, 1978; El Gomati et al., 1979). However, as Cazaux (1983) has emphasized, if high-quality quantitative analysis is desired, the effective sampling area may have to be considered substantially larger than implied by El Gomati and others.

Charging and charge-neutralization methods

It has been known for some time that insulating surfaces under electron-beam bombardment can remain neutral or even charge positively under certain beam conditions (Bruining, 1954). For an electron beam impinging on an insulating surface, charge neutralization is achieved when

$$I_p = I_\gamma + I_\delta + I_A,$$

where I_p is the primary electron-beam current, I_γ is the electron current produced by primary backscattered electrons and target electrons ejected by the primary beam with energies above approximately 50 eV, I_δ is the secondary electron current (energies below 50 eV), and I_A is the current of all Auger electrons coming from the sample. I_A is very small compared to I_γ and I_δ and can be neglected. Unfortunately, at a constant I_p, decreasing the accelerating potential of the primary beam, E_p, has little effect on I_γ (see Goldstein et al., 1981). However, I_δ is dependent on E_p (see, e.g., Dawson, 1966, and Koshikawa and Shimizu, 1974) as shown in Figure 3. Therefore, by adjusting E_p, I_δ can be varied, and a stable charging situation will exist when either I_p is equal to or slightly less than $I_\gamma + I_\delta$. If I_p is greater than $I_\gamma + I_\delta$, the negatively charged surface results in Auger peaks that are shifted to higher energies. At excessive I_p, the surface charge is unstable resulting in unusable spectra.

For insulators, the "crossover voltages" E_I and E_{II}, where $I_p = I_\gamma + I_\delta$ (Fig. 3), typically differ by a few thousand electron volts, and E_I is usually only a few tens of volts

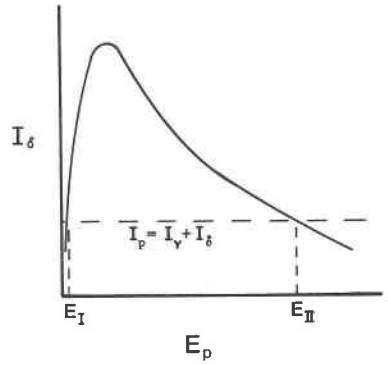

Fig. 3. Secondary electron emission (I_δ) as a function of primary electron-beam energy (E_p) for an insulator. E_I and E_{II} are the crossover voltages where the primary beam current (I_p) is equal to the backscattered electron current (I_γ) plus the secondary electron current (I_δ), and no charging will occur.

(Dawson, 1966), far too low to be useful in AES. Most Auger work on insulators is performed near E_{II}, which is typically between 2 and 5 keV.

It has also been known for some time that tilting the sample in relation to the primary beam permits the collection of unshifted Auger spectra at higher E_p than could be achieved with an untilted specimen. Tilting the sample results in an increase in both the backscattered and secondary emission efficiency for any particular beam energy (Kanter, 1961; Newbury et al., 1973). A high E_p may be necessary in order to obtain a reasonable signal-to-noise ratio for certain Auger lines although, generally, the probability of Auger transitions does not increase with increasing E_p over 3 keV. (Davis et al., 1976; Joshi et al., 1975, and references therein.)

There are two relatively new charge-neutralization techniques that have as yet met with only limited success, although they may become useful with further development. The first involves accelerating low-energy (10 eV) Ar^+ ions at the sample during electron bombardment.[1] This method has been shown to dramatically improve SEM images of uncoated insulating surfaces (Crawford, 1979, 1980). At these low energies, no sputtering occurs, but it is difficult to focus a low-energy ion beam, and the positive-charge density has not been sufficient to counteract the negative-charge density resulting from high-resolution SAM. The other charge-neutralization technique involves using ultrathin samples,[2] the idea being that many primary electrons will travel through the sample to a supporting conductor and charge neutralization will not be solely dependent on I_γ and I_δ. Further advances in the ultramicrotome cutting of brittle materials may make this a viable technique for charge reduction.

[1] This work has been primarily performed by S. Clough and D. Paul at the Perkin-Elmer, Physical Electronics Laboratory in Eden Prairie, Minnesota.

[2] This work was performed by D. Pickles and M. Hochella at Corning Glass Works, Corning, New York.

Finally, sample charging also depends on the specific dielectric properties of the material under investigation, beam-current density, and surface contamination and roughness, all of which should be considered for each analysis. For example, although not always predictable, we have found that it is generally more difficult to obtain usable uncharged spectra on rougher surfaces. This can be rationalized by realizing that the beam will be impinging on the surface of a rough sample at many angles, many not appropriate for the beam conditions used.

Quantification

Quantitative analysis of solid near-surfaces by AES has been under development since the early 1970s. Palmberg (1973) was among the first to outline the theory of quantitative analysis using AES. Reviews of some of the more recent work can be found in Powell (1980), Prutton (1982), and Seah (1983).

Considering the fact that the physical mechanisms of the processes resulting in AES are closely related to those responsible for electron-stimulated X-ray fluorescence, the potential and relative ease of quantitative analysis of both should be similar. Sekine et al. (1983) have proposed a model for quantitative Auger analysis somewhat analogous to the ZAF corrections used in conjunction with quantitative EPMA analysis. However, quantification for AES is not yet as advanced as for EPMA. Part of the problem stems from an incomplete understanding of the matrix effects of electron-escape depth (see Powell, 1984, and references therein) and backscattering phenomenon (Ichimura et al., 1983). Other areas of difficulty deal with understanding consequences of electron-beam damage on surfaces (Levenson, 1982), anisotropic Auger emission from different crystallographic orientations (Armitage et al., 1980, and references therein; Le Gressus et al., 1983), and rough surfaces (deBernardez et al., 1984; Wehbi and Roques-Carmes, 1985).

Semiquantitative to quantitative chemical analysis by AES is most easily done directly with standards (see, e.g., Seah, 1983, and Moon and Bishop, 1984) or with sensitivity factors derived from standards (Davis et al., 1976; Mroczkowski and Lichtman, 1983; Payling, 1985). Owing to matrix effects, it is possible that large errors can be made when the standards are not similar to the unknowns. Sensitivity factors specifically for silicates and geologically important oxides are now becoming available. Kovacich and Lichtman (1985) measured Auger intensities and derived sensitivity factors for silica, alumina, and two aluminosilicates. Sensitivity factors for a number of the most common elements in the rock-forming minerals will be reported in a future paper in this series.

Demonstration of the technique

The following is an example of analyzing and identifying a <1-μm grain in a rock with SAM. Actual application of SAM to geologic research will be detailed in subsequent papers in this series. The rock sample used in this example is from the gold-bearing carbonate strata of the Roberts Mountains Formation near Carlin, Nevada. Detailed description of this ore body can be found in Hausen and Kerr (1968) and Wells and Mullens (1973). The particular specimen chosen is a carbonaceous silty limestone containing fine pyrite. The <1-μm grains examined in this rock and described below are on pyrite surfaces.

Sample preparation and run conditions

The sample surface studied was exposed by fracturing in air. The sample was degreased by boiling for 2 min each in reagent-grade acetone and ethanol. It was then mechanically secured onto a stainless-steel platform and degaussed before entry into the instrument. The sample stage was tilted such that the angle between the sample normal and the electron-beam direction was between 40 and 60°.

Vacuum during data collection was between 10^{-9} and 10^{-10} torr. For Auger data collection, a 3-keV beam was used, giving a sample current of approximately 10 nA. Beam current was not measured directly. The beam diameter during Auger analysis was estimated to be 0.2 μm in diameter. Beam conditions for SEM imaging ranged from 3 to 5 keV and typically less than 1 nA, resulting in a beam approximately 0.05 μm in diameter.

Results

In our specimens, the pyrite grains are euhedral and 0.1 mm or less on a side. An SEM micrograph (taken using the Phi 600 SAM) of an uncoated specimen is shown in Figure 4A. An Auger spectrum of a general area of this pyrite surface shows Fe and O with minor Ca, S, Si, K, and C (Fig. 5A). Although the major low-energy Fe Auger line (47 eV) would mask a smaller Al signal (51 eV), there is no evidence for Al at 1378 eV, the position of the major high-energy Al Auger line (not shown). Sputtering the surface with 3 keV Ar^+ ions for 4 min showed a dramatic decrease in O and increase in S, as expected (Fig. 5B). The observance of the Si, K, and Ca in the Auger spectra described above is the result of the tiny grains on the pyrite surface that are visible in Figure 4A and magnified in Figure 4B. The crystals appear to be generally tabular, <1 μm in overall dimension, and approximately 0.2 μm thick. The Auger spectrum taken on one of these crystals (Fig. 6) shows major O, Si, K, Ca, and minor F. Using the Auger sensitivity factors of Davis et al. (1976), the mineral can be identified as apophyllite, $KCa_4Si_8O_{20}(F,OH)\cdot 8H_2O$ (see Table 2). Apophyllite has not been described in these rocks before, perhaps because of its minute size. However, it has been found previously in somewhat similar settings, i.e., in limestones associated with sulfide mineralization (Sahama, 1965; Roberts et al., 1974). The two Auger spectra in Figure 5 further imply that the pyrite surface is an iron oxide (the O/Fe line intensity ratios suggest Fe_2O_3) and that, after a few hundred ångströms of surface removal,[3] we are in the vicinity of the oxide-sulfide or sul-

[3] Although the sputtering rates for our ion gun have not been calibrated specifically for iron oxides, sulfates, and sulfides, we anticipate sample-surface removal of between 50 and 150 Å/min.

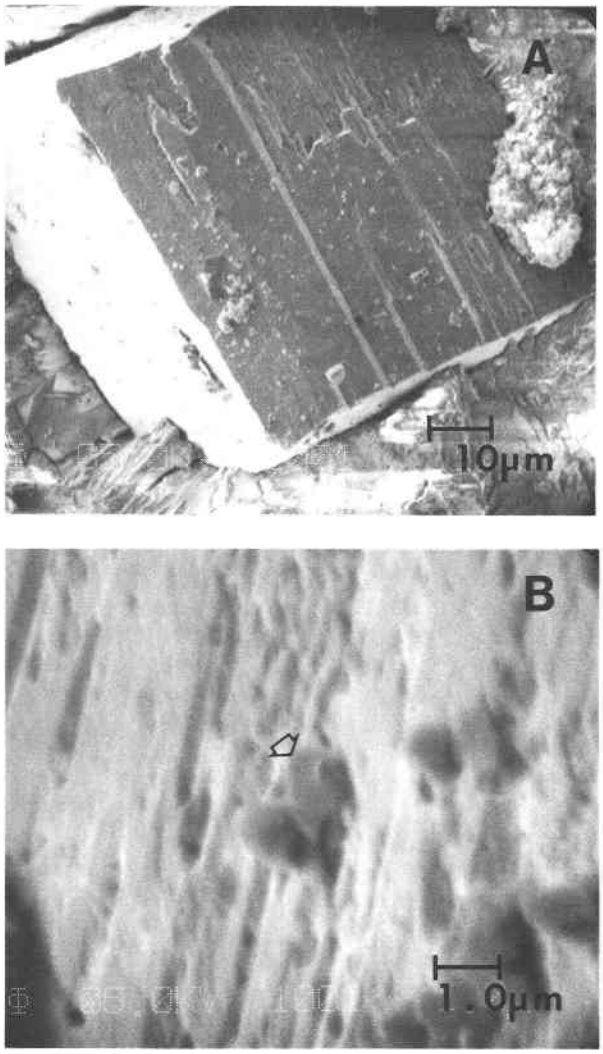

Fig. 4. SEM micrographs of an uncoated specimen of a carbonaceous silty limestone from the gold-bearing strata of the Roberts Mountains Formation near Carlin, Nevada. (A) Euhedral pyrite grain, approximately 70 μm on an edge, with <1-μm apophyllite grains dotting the surface. (B) High-magnification image of several tabular apophyllite grains on the pyrite surface. The arrow marks a single apophyllite grain that was analyzed (see Fig. 6 and Table 2).

fate-sulfide interface. Further experiments would be required to determine the presence of a sulfate layer between the oxide and sulfide [see Perry et al. (1983b, 1984a) for a discussion of this type of investigation on galena and sphalerite surfaces].

Discussion

The near-surface microanalysis capability of high-resolution SAM makes it suitable for semiquantitative probing of <1-μm mineral grains as well as performing surface studies with very high lateral resolution. However, it is critical to constantly consider potential electron-beam degradation effects such as field-induced ion migration,

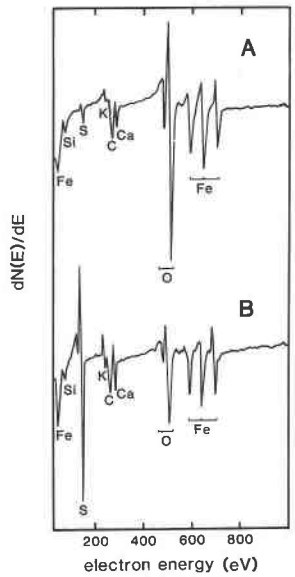

Fig. 5. Differentiated Auger spectra of the pyrite surface shown in Fig. 4A before sputtering (A) and after 4 min of sputtering with Ar^+ ions at 3 kV (B). See text for explanation.

beam heating, and electron-stimulated desorption and adsorption (ESD and ESA, respectively). The lighter alkalis, particularly Li and Na, can migrate within a matter of seconds from the analysis area (Dawson et al., 1978; Gossink et al., 1980); beam heating and ESD can break down carbonates (Storp, 1985; Mossotti et al., 1986); even oxygen will desorb from the surface of oxides and silicates subjected to excessive beam-current densities (Carriere and Lang, 1977). Reviews of electron-beam damage during AES analysis for materials in general are given in Pantano and Madey (1981) and Levenson (1982).

In this study, beam damage and ion migration were kept to a minimum by using very low beam currents and voltages and rastering or defocusing the beam whenever

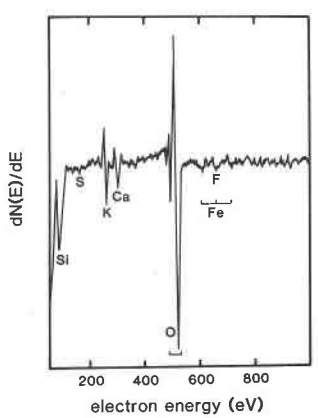

Fig. 6. Differentiated Auger spectrum of the <1-μm apophyllite grain marked by an arrow in Fig. 4B. Fe and S Auger peaks, due to the nearby pyrite surface, are barely distinguishable in this spectrum. A chemical analysis derived from this spectrum is listed in Table 2.

Table 2. Semiquantitative analysis of <1-μm apophyllite grain (Fig. 4B)

Element	Sensitivity factor*	Peak-to-peak height	Atomic proportion (%)†	Apophyllite chemistry‡
O	0.42	116	63	68
Si	0.30	26	20	20
K	0.95	28	7	2
Ca	0.40	17	10	10

* Obtained from Davis et al. (1976).
† Peak-to-peak height divided by sensitivity factor and normalized to 100.
‡ H and F have been excluded.

possible. Beam currents and voltages were set only high enough so that adequate signal-to-noise ratios could be obtained within a reasonable time. Beam damage is most readily apparent when spectra are not reproducible, or, for silicates, when an Auger line appears at 92 eV, indicative of reduced Si due to the electron-stimulated desorption of oxygen. Electron-beam damage was not noticeable for the minerals probed in this study when run under the conditions described above.

The Auger spectrum taken on one of the apophyllite grains (Fig. 6) is particularly helpful in establishing the high analytic resolution possible with SAM even on insulating materials. Although the beam had to be positioned on the apophyllite crystal less than 0.5 μm from the pyrite surface, there are only traces of Fe and S Auger lines in the spectrum (Fig. 6), barely distinguishable in the background. This result is perhaps surprising because the analyzed apophyllite surface and the pyrite surface are at approximately right angles to one another (Fig. 4B). Some of the primary elastically scattered and backscattered electrons from the apophyllite grain must have been impinging on the pyrite surface. This is probably the origin of the minute S and Fe lines. What may be even more remarkable is the chemistry derived from the apophyllite spectra (Table 2). The chemistry is remarkedly close to the ideal apophyllite formula, excluding K, considering that the sensitivity factors used were derived from the pure elements or simple compounds on another spectrometer with slightly different electron-transmission characteristics than the Phi 600. Our preliminary results for sensitivity factors derived from silicate standards indicate that large discrepancies in calculated chemistries, as in the case of K in apophyllite, will disappear.

Conclusions

In this study, SAM has demonstrated analytic lateral resolution for minerals better than 1 μm. The results of Hochella et al. (1986) indicate that lateral resolution for insulators in the neighborhood of 0.1 μm is possible under certain conditions. The depth resolution of no more than a few tens of ångströms is orders of magnitude better than the electron microprobe, and the sensitivity of SAM for light elements is also extremely important. The largest drawback in using SAM as a high-resolution microprobe on insulating surfaces is the charging problem. Conductive coatings, as are used with the electron microprobe, would have to be exceedingly thin given the extreme depth resolution of Auger spectroscopy. For many surfaces and potential coating materials, it is difficult to deposit a continuous layer that is sufficiently thin, especially if the surface is rough. However, as explained above, certain beam conditions and tilt angles can prevent charging. It has been our experience that the instrument and sample conditions under which a reasonable signal-to-noise ratio can be achieved for small spot AES/SAM of silicate, oxide, and sulfide surfaces without charging or significant sample degradation are as follows: (1) beam voltage typically 3 keV, but no higher than 5 keV; (2) for <1-μm beam diameters, beam currents between approximately 1 and 20 nA; (3) tilt angle typically between 40 and 60°; (4) flat to semirough surfaces; and (5) light C, CO, CO_2 atmospheric contamination, sometimes resulting in a weak C Auger line in the spectrum.

Finally, we have compared SAM with three electron-beam microanalytic techniques that are commonly used in geologic research today, namely EPMA, SEM/EDS, and STEM/EDS (Table 3). As can be seen, the major disadvantages of SAM in this context are the potential sample-charging problems, its sensitivity to electron-beam-stimulated surface degradation, and with respect to EPMA, its current shortcomings in quantitative analysis. The major advantages of SAM over EPMA and SEM/EDS are greater lateral and depth analytic resolution and ease of light-element detection. Its major advantages over STEM/EDS are ease of sample preparation and light-element detection. However, despite their advantages and disadvantages, it is

Table 3. Commonly used microanalysis techniques compared with SAM

	EPMA	SEM/EDS	STEM/EDS	SAM
Lightest detectable element	Be*	Be*	Be*	Li
Best lateral spatial resolution for chemical analysis	1–2 μm†	1–2 μm†	0.005 μm	0.030 μm
Depth resolution for chemical analysis	1–3 μm†	1–3 μm†	sample thickness	0.003 μm‡
Quantification	quant.	semiquant.	semiquant.	semiquant.
Sample-charging problems	none	few	none	can be significant
Sample preparation	polish and sputter coat	sput. coat	ultra-thin sample	high-vacuum compatible

* Detection of elements lighter than Na requires a thin-window (for EPMA and EDS) or a windowless (for EDS) X-ray detector.
† Estimated for oxides with beam voltages in the range 10–15 keV.
‡ Estimated for oxides.

becoming increasingly apparent that all of these microanalysis techniques will become even more important in future fundamental and applied geologic research as interest in the extremely fine features in rocks continues to grow.

Acknowledgments

M.F.H. is sincerely grateful to the Perkin-Elmer Corporation, Physical Electronics Division, for making this project possible. G. E. Brown, Jr., of Stanford, B.H.W.S. deJong of Corning Glass, and R. G. Burns of MIT provided reviews that were extremely helpful. We also wish to thank M. T. Einaudi and B. M. Bakken of Stanford for providing the Carlin ore samples and for helpful discussions concerning these rocks.

References

Armitage, A.F., Woodruff, D.P., and Johnson, P.D. (1980) Crystallographic incident beam effects in quantitative Auger electron spectroscopy. Surface Science, 100, L483–L490.

Auger, P. (1975) The Auger effect. Surface Science, 48, 1–8.

Baron, R.L., Bilson, E., Gold, T., Colton, R.J., Hapke, B., and Steggert, M.A. (1977) The surface composition of lunar soil grains: A comparison of the results of Auger and X-ray photoelectron (ESCA) spectroscopy. Earth and Planetary Science Letters, 37, 263–272.

Bisdom, E.B.A., Henstra, S., Kooistra, M.J., van Ooij, W.J., and Visser, T.H. (1985) Combined high-resolution scanning Auger microscopy and energy dispersive x-ray analysis of soil samples. Spectrochimica Acta, 40B, 879–884.

Bruining, H. (1954) Physics and applications of secondary electron emission. Pergamon Press, London.

Burhop, E.H.S. (1952) The Auger effect and other radiationless transitions. Cambridge University Press, Cambridge.

Carriere, B., and Lang, B. (1977) A study of the charging and dissociation of SiO_2 surfaces by AES. Surface Science, 64, 209–223.

Carriere, B., Deville, J-P., and Goldsztaub, S. (1973) Auger electron spectroscopy of insulating silicon compounds. Vacuum, 22, 485–487.

Castaing, R. (1960) Electron probe microanalysis. Advances in Electronics and Electron Physics, 13, 317–386.

Cazaux, J. (1983) Mathematical and physical considerations on the spatial resolution in scanning Auger electron microscopy. Surface Science, 125, 335–354.

——— (1984) Detection limits in Auger electron spectroscopy. Surface Science, 140, 85–100.

Chang, C. C. (1971) Auger electron spectroscopy. Surface Science, 25, 53–79.

Coghlan, W.A., and Clausing, R.E. (1971) A catalog of calculated Auger transitions for the elements. Oak Ridge National Laboratory, Technical Manuscript 3576.

Connell, G.L., Schneidmiller, R.F., Kraatz, P., and Gupta, Y.P. (1971) Auger electron spectroscopy of lunar materials. Proceedings of the Second Lunar Science Conference, Geochimica et Cosmochimica Acta, Supplement 3, 2, 2083–2092.

Crawford, C.K. (1979) Charge neutralization using very low energy ions. Scanning Electron Microscopy, 1979, 31–46.

——— (1980) Ion charge neutralization effects in scanning electron microscopes. Scanning Electron Microscopy, 1980, 11–25.

Davis, L.E., MacDonald, N.C., Palmberg, P.W., Riach, G.E., and Weber, R.E. (1976) Handbook of Auger electron spectroscopy, 2nd edition. Physical Electronics Division, Eden Prairie, Minnesota.

Dawson, P.H. (1966) Secondary electron emission yields of some ceramics. Journal of Applied Physics, 37, 3644–3645.

Dawson, P.T., Heavens, O.S., and Pollard, A.M. (1978) Glass surface analysis by Auger electron spectroscopy. Journal of Physics C: Solid State Physics, 11, 2183–2193.

deBernardez, L.S., Ferron, J., Goldberg, E.C., and Buitrago, R.H. (1984) The effect of surface roughness on XPS and AES. Surface Science, 139, 541–548.

El Gomati, M.M., and Prutton, M. (1978) Monte Carlo calculations of the spatial resolution in a scanning Auger electron microscope. Surface Science, 72, 485–494.

El Gomati, M.M., Janssen, A.P., Prutton, M., and Venables, J.A. (1979) The interpretation of the spatial resolution of the scanning Auger electron microscope. Surface Science, 85, 309–316.

Gold, T., Bilson, E., and Baron, R.L. (1974) Observation of iron-rich coating on lunar grains and a relation to low albedo. Proceedings of the Fifth Lunar Conference, Geochimica et Cosmochimica Acta, Supplement 5, 3, 2413–2422.

——— (1975) Auger analysis of the lunar soil: Study of processes which change the surface chemistry and albedo. Proceedings of the Sixth Lunar Science Conference, Geochimica et Cosmochimica Acta, Supplement 6, 3, 3285–3303.

Goldstein, J.I., Newbury, D.E., Echlin, P., Joy, D.C., Fiori, C., and Lifshin, E. (1981) Scanning electron microscopy and X-ray microanalysis. Plenum Press, New York.

Gossink, R.G., van Doveren, H., and Verhoeven, J.A.T. (1980) Decrease of the alkali signal during Auger analysis of glasses. Journal of Non-Crystalline Solids, 37, 111–124.

Grant, R.W., Housley, R.M., Szalkowski, F.J., and Marcus, H.L. (1974) Auger electron spectroscopy of lunar samples. Proceedings of the Fifth Lunar Conference, Geochimica et Cosmochimica Acta, Supplement 5, 3, 2423–2439.

Harris, D.W. (1984) Surfaces, science . . . fact, not fiction. Solid State Technology, 27, 278–285.

Hausen, D.M., and Kerr, P.F. (1968) Fine gold occurrence at Carlin, Nevada. In J.D. Ridge, Ed. Ore deposits of the United States, 1933–1967, p. 908–940. American Institute of Mining, Metallurgical and Petroleum Engineers, New York.

Hillier, J. (1943) On microanalysis by electrons. Physics Review, 64, 318.

Hochella, M.F., Jr. (1985) Development of scanning Auger microscopy as a high resolution microprobe for geologic materials. EOS (American Geophysical Union Transactions), 66, 407–408.

Hochella, M.F., Jr., Harris, D.W., and Turner, A.M. (1985) Scanning Auger microscopy: Development and applications for geologic materials. Geological Society of America Abstracts with Programs, 17, 611.

Hochella, M.F., Jr., Turner, A.M., and Harris, D.W. (1986) High resolution scanning Auger microscopy of mineral surfaces. Scanning Electron Microscopy, 1986, 337–349.

Holloway, P.H. (1980) Applications of surface analysis for electronic devices. Applications of Surface Analysis ASTM STP, 1980, 5–23.

Holm, R. (1982) Some applications of Auger microanalysis in the chemical industry. Scanning Electron Microscopy, 1982, 1043–1052.

Ichimura, S., Shimizu, R., and Langeron, J.P. (1983) Backscattering correction for quantitative Auger analysis. III. A simple functional representation of electron backscattering factors. Surface Science, 124, L49–L54.

Janssen, A.P., and Venables, J.A. (1978) The effect of backscattered electrons on the resolution of scanning Auger microscopy. Surface Science, 77, 351–364.

Joshi, A., Davis, L.E., and Palmberg, P.W. (1975) Auger electron spectroscopy. In A.W. Czanderna, Ed. Methods of surface analysis, 159–222. Elsevier, New York.

Kanter, H. (1961) Energy dissipation and secondary electron emission in solids. Physical Review, 121, 677–681.

Koshikawa, T., and Shimizu, R. (1974) A Monte Carlo calculation of low-energy secondary electron emission from metals. Journal of Physics D: Applied Physics, 7, 1303–1315.

Kovacich, J.A., and Lichtman, D. (1985) A qualitative and quantitative study of the oxides of aluminum and silicon using AES

and XPS. Journal of Electron Spectroscopy and Related Phenomena, 35, 7–18.

Lander, J.J. (1953) Auger peaks in the energy spectra of secondary electrons from various materials. Physical Review, 91, 1382–1387.

Larkins, F.P. (1977) Semiempirical Auger-electron energies for elements $10 < Z < 100$. Atomic Data Nuclear Data Tables, 20, 311–387.

Le Gressus, C., Duraud, J.P., Massignon, D., and Lee-Deacon, O. (1983) Electron channelling effect on secondary electron image contrast. Scanning Electron Microscopy, 1983, 537–542.

Levenson, L.L. (1982) Electron beam–solid interactions: Implications for high spatial resolution Auger electron spectroscopy. Scanning Electron Spectroscopy, 1982, 925–936.

Lowry, R.K., and Hogrefe, A.W. (1980) Applications of Auger and photo-electron spectroscopy in characterizing IC materials. Solid State Technology, 1980, 71–75.

MacDonald, N.C. (1970) Auger electron spectroscopy in scanning electron microscopy: Potential measurements. Applied Physics Letters, 16, 76–80.

Mackinnon, I.D.R., and Mogk, D.W. (1985) Surface sulfur measurements on stratospheric particles. Geophysical Research Letters, 12, 93–96.

Mogk, D.W., Mackinnon, I.D.R., and Rietmeijer, F.J.M. (1985) Auger spectroscopy of stratospheric particles: The influence of aerosols on interplanetary dust. Journal of Geophysical Research, Proceedings of the Sixteenth Lunar and Planetary Science Conference, Part I, 30–31.

Moon, D.P., and Bishop, H.E. (1984) Determination of elemental intensities from direct Auger spectra by pre-filtered least squares fitting. Scanning Electron Microscopy, 1984, 1203–1210.

Morrison, G.H., Gerard, J.T., Kashuba, A.T., Rothenberg, E.V., Potter, N.M., and Miller, G.B. (1970) Elemental abundances of lunar soil and rocks. Proceedings of the Apollo 11 Lunar Science Conference, Geochimica et Cosmochimica Acta, Supplement 1, 2, 1383–1392.

Mossotti, V.G., Lindsay, J.R., and Hochella, M.F., Jr. (1986) Surface characterization of Salem limestone as a control material in acid rain weathering. U.S. Geological Survey Open-File Report, 86-336, 25 p.

Mroczkowski, S., and Lichtman, D. (1983) Calculated Auger sensitivity factors compared to experimental handbook values. Surface Science,131, 159–166.

Mucci, A., and Morse, J.W. (1985) Auger spectroscopy determination of the surface-most adsorbed layer composition on aragonite, calcite, dolomite, and magnesite in synthetic seawater. American Journal of Science, 285, 306–317.

Mucci, A., Morse, J.W., and Kaminsky, M.S. (1985) Auger spectroscopy analysis of magnesian calcite overgrowths precipitated from seawater and solutions of similar composition. American Journal of Science, 285, 289–305.

Newbury, D.E., Yakowitz, H., and Myklebust, R.L. (1973) Monte Carlo calculations of magnetic contrast from cubic materials in the scanning electron microscope. Applied Physics Letters, 23, 488–490.

Ohuchi, F., Clark, D.E., and Hench, L.L. (1979) Effect of crystallization on the Auger electron signal decay in an $Li_2O \cdot 2SiO_2$ glass and glass-ceramic. American Ceramic Society Journal, 62, 500–503.

Olson, R.R., Palmberg, P.W., Hovland, C.T., and Brady, T.E. (1983) Applications of AES in microelectronics. In D. Briggs and M.P. Seah, Eds. Practical surface analysis by Auger and X-ray photoelectron spectroscopy, 217–246. John Wiley and Sons, New York.

Palmberg, P.W. (1973) Quantitative analysis of solid surfaces by Auger electron spectroscopy. Analytical Chemistry, 45, 549A–556A.

Palmberg, P.W., Bohn, G.K., and Tracy, J.C. (1969) High sensitivity Auger electron spectrometer. Applied Physics Letters, 15, 254–255.

Pantano, C.G. (1981) Surface and in-depth analysis of glass and ceramics. Ceramic Bulletin, 60, 1154–1167.

Pantano, C.G., and Madey, T.E. (1981) Electron beam damage in Auger electron spectroscopy. Applications of Surface Science, 7, 115–141.

Pantano, C.G., Dove, D.B., and Onoda, G.Y. (1975) Glass surface analysis by Auger electron spectroscopy. Journal of Non-Crystalline Solids, 19, 41–53.

Payling, R. (1985) Modified elemental sensitivity factors for Auger electron spectroscopy. Journal of Electron Spectroscopy and Related Phenomena, 36, 99–104.

Perry, D.L., Tsao, L., Gaugler, K.A., and Taylor, J.A. (1982a) Studies of the bonding of iron on feldspar surfaces using X-ray photoelectron spectroscopy, scanning electron microscopy, and scanning Auger microscopy. Book of Abstracts, 184th American Chemical Society National Meeting, Division of Geochemistry, abstract 27.

Perry, D.L., Tsao, L., and Gaugler, K.A. (1982b) Studies of the bonding of cobalt on feldspar surfaces using X-ray photoelectron spectroscopy (XPS), scanning electron microscopy (SEM), and scanning Auger microscopy (SAM). 1982 Annual Meeting of the Materials Research Society Abstracts, Symposium D. Boston, Massachusetts.

——— (1983a) Surface study of HF- and HF/H_2SO_4-treated feldspar using Auger electron spectroscopy. Geochimica et Cosmochimica Acta, 47, 1289–1291.

Perry, D.L., Tsao, L., and Taylor, J.A. (1983b) Surface studies of galena (PbS) using X-ray photoelectron spectroscopy and scanning Auger microscopy. Book of Abstracts, 185th American Chemical Society National Meeting, Division of Geochemistry, abstract 82.

——— (1984a) Surface studies of the interaction of copper ions with metal sulfide minerals. Electrochemical Society, Extended Abstracts, 84-1, 363.

——— (1984b) The galena/dichromate solution interaction and the nature of the resulting chromium(III) species. Inorganica Chimica Acta, 85, L57–L60.

Poppa, H., and Elliot, A.G. (1971) The surface composition of mica substrates. Surface Science, 24, 149–163.

Powell, C.J. (1980) Quantification of surface analysis techniques. Applied Surface Science, 4, 492–511.

——— (1984) Inelastic mean free paths and attenuation lengths of low-energy electrons in solids. Scanning Electron Microscopy, 1984, 1649–1664.

Prutton, M. (1982) How quantitative is analysis in the scanning Auger electron microscope?. Scanning Electron Microscopy, 1982, 83–91.

Remond, G., Holloway, P.H., and Gressus, C. (1981) Electron spectroscopy and microscopy for studying surface changes of mechanically prepared pyrite and quartz. Scanning Electron Microscopy, 1981, 483–492.

Remond, G., Holloway, P.H., Hovland, C.T., and Olson, R.R. (1982) Bulk and surface silver diffusion related to tarnishing of sulfides. Scanning Electron Microscopy, 1982, 995–1011.

Remond, G., Picot, P., Giraud, R., Holloway, P.H., and Ruzakowski, P. (1983) Contribution of electron spectroscopies to X-ray spectroscopy applied to the geosciences. Scanning Electron Microscopy, 1983, 1683–1706.

Remond, G., Holloway, P.H., Kosakevitch, A., Ruzakowski, P., Packwood, R.H., and Taylor, R.A. (1985) X-ray spectrometry, electron spectroscopies and optical microreflectometry applied to the study of ZnS tarnishing in polished sulfide ore specimens. Scanning Electron Microscopy, 1985, 1305–1326.

Riviere, J.C. (1983) Auger techniques in analytic chemistry. The Analyst, 108, 649–684.

Roberts, W. L., Rapp, G.R., and Weber, J. (1974) Encyclopedia of minerals. Van Nostrand Reinhold, New York.

Ruthemann, G. (1942) Elektronenbremsung an rontgenniveaus. Nafurwissenscheften, 30, 145.

Sahama, Th.G. (1965) Yellow apophyllite from Korsnas, Finland. Mineralogical Magazine, 34, 406–415.

Schowengerdt, F.D., and Forrest, J.S. (1983) Chemical effects in the analysis of lithium compounds by Auger electron spectroscopy. Scanning Electron Microscopy, 1983, 543–551.

Seah, M.P. (1979) Quantitative Auger electron spectroscopy: Via the energy spectrum or the differential? Surface and Interface Analysis, 1, 86–90.

——— (1983) A review of quantitative Auger electron spectroscopy. Scanning Electron Microscopy, 1983, 521–536.

Seah, M.P., and Dench, W.A. (1979) Quantitative electron spectroscopy of surfaces: A standard data base for electron inelastic mean free paths in solids. Surface and Interface Analysis, 1, 2–11.

Sekine, T., Hirata, K., and Mogami, A. (1983) Matrix effect correction in quantitative Auger electron spectroscopy. Surface Science, 125, 565–574.

Shaffner, T.J., and Keenan, J.A. (1983) Some limits of sensitivity enhancement in Auger microscopy. Scanning Electron Microscopy, 1983, 1107–1114.

Shirley, D.A. (1972) Relaxation effects on Auger energies. Chemical Physics Letters, 17, 312–315.

Stephenson, D.A., and Binkowski, N.J. (1976) X-ray photoelectron spectroscopy of silica in theory and experiment. Journal of Non-Crystalline Solids, 22, 399–421.

Storp, S. (1985) Radiation damage during surface analysis. Spectrochimica Acta, 40B, 745–756.

Thompson, M., Baker, M.D., Christie, A., and Tyson, J. (1985) Auger electron spectroscopy. Wiley, New York.

Venables, J.A., Janssen, A.P., Harland, C.J., and Joyce, B.A. (1976) Scanning Auger electron microscopy at 30 nm resolution. Philosophical Magazine, 34, 495–500.

Wagner, C.D., Passoja, D.E., Hillery, H.F., Kinisky, T.G., Six, H.A., Jansen, W.T., and Taylor, J.A. (1982) Auger and photoelectron line energy relationships in aluminum-oxygen and silicon-oxygen compounds. Journal of Vacuum Science and Technology, 21, 933–944.

Wehbi, D., and Roques-Carmes, C. (1985) Surface roughness contribution to the Auger electron emission. Scanning Electron Microscopy, 1985, 171–177.

Wells, J.D., and Mullens, T.E. (1973) Gold-bearing arsenian pyrite determined by microprobe analysis, Cortez and Carlin gold mines, Nevada. Economic Geology, 68, 187–201.

Wells, O.C., and Bremer, C.G. (1969) Improved energy analyser for the scanning electron microscope. Journal of Scientific Instrumentation (Journal of Physics E), 2, 1120–1121.

White, A.F., and Yee, A. (1985) Aqueous oxidation-reduction kinetics associated with coupled electron-cation transfer from iron-containing silicates at 25°C. Geochimica et Cosmochimica Acta, 49, 1263–1275.

Manuscript received October 24, 1985
Manuscript accepted May 16, 1986